Analysis of M-ary Phase-Shift Keying with Diversity Reception for Land-Mobile Satellite Channels

C. Tellambura, A. Joseph Mueller, and Vijay K. Bhargava, *Fellow, IEEE*

***Abstract*— An analytical technique well suited to numerical analysis is presented for computing the average bit-error rate (BER) and outage probability of M-ary phase-shift keying (PSK) in the land-mobile satellite channel (LMSC) with microdiversity reception. Closed-form expressions are found for L-branch microdiversity using both selection diversity combining (SDC) and maximal ratio combining (MRC). These expressions are extended to include both M-ary coherent PSK (M-PSK) and differential PSK [M-differential PSK (DPSK)]. Following previous empirical studies, the LMSC is modeled as a weighted sum of Rice and Suzuki distributions. Numerical results are provided illustrating the achievable performance of both M-PSK and M-DPSK with diversity reception. Using measured channel parameters, the performance in various mobile environments for various satellite elevation angles is also found.**

***Index Terms*—Diversity methods, fading channels, land-mobile radio, phase-shift keying.**

I. Introduction

With the growing interest in satellite communications to provide personal communications services (PCS's), the importance of exact theoretical analysis for such systems hardly needs to be stated. Particularly important are exact analytical expressions for the bit-error rate (BER) and outage probability required to design effective signaling and error control coding schemes. Furthermore, a consequence of the exploding demand for mobile communications services is the need to provide a large number of users with such services despite the limited radio spectrum. This warrants a consideration of modulation methods with large constellation sizes (≥ 4), leading to systems with higher bandwidth efficiency. Moreover, since the received signal suffers from multipath fading, diversity reception can be employed to alleviate such fading effects. In light of these considerations, this paper takes an analytical approach to study the performance of such communications systems in the land-mobile satellite channel (LMSC).

Typically, for the LMSC, the amplitude fading of the received signals is described by a Rician distribution. This fading makes carrier recovery more difficult and introduces an irreducible error floor. When the line-of-sight (LOS) component of the received signal vanishes, the Rician distribution degenerates to the Rayleigh distribution. Signal shadowing (i.e., large-area variations of the mean power of the signals) occurs due to obstacles in the terrain and is commonly described by lognormal statistics. Since a mobile can rapidly move from a shadowed reception area to an unshadowed one, it is worthwhile to consider a composite model, where the received signal consists of a weighted sum of shadowed and unshadowed signals. It is this relatively unexplored model that we now describe.

A previous study [1] suggests a composite model based on empirical measurements for the fading of the received signal in the LMSC. The channel can be in a "good" or "bad" state a fraction of the time. The fading in the "good" state is relatively benign and is represented by a Rician distribution. The fading in the "bad" state is modeled by a Rayleigh distribution superimposed on a lognormal distribution, known as a Suzuki distribution [3]. Furthermore, in [1] an analytical solution is derived showing the BER for binary differential phase-shift keying (DPSK) and noncoherent frequency-shift keying (FSK) over this channel (although the solution is mathematically complex). The channel cutoff rate for this model is evaluated in [4], where several other papers that address this composite channel model are also mentioned. In other work [5], exact expressions for the BER for M-ary PSK and DPSK in a slow fading Rayleigh channel without diversity were obtained.

In our previous work [6], we extended the study [1] in several ways: 1) by exploiting the properties of the moment generating function (MGF), a computationally simple formula for the BER was derived; 2) the BER formula was generalized for L-branch MRC microdiversity; and 3) the outage probability was determined. Again, by exploiting the MGF properties, this work continues [6] by integrating the BER expressions for M-ary PSK and DPSK in [5] with the channel model proposed in [1].

While there are many excellent papers on the subject of fading channels, with many cases having been thoroughly analyzed, the approach we have taken in this paper results in "clean" derivations for BER expressions and numerically efficient solutions. As stated above, one important technique recurring throughout the paper is the use of MGF's to obtain the BER expressions. For coherent or differential detection of MPSK signals, the instantaneous BER can be expressed as $g(\exp(-kS))$, where k is some factor, S is the signal power, and $g(x)$ is a certain function. For instance, $g(x) = x/2$ for binary DPSK. Now, we are primarily interested in the

Manuscript received June 5, 1995; revised October 25, 1996. This work was supported by the Natural Sciences and Engineering Council of Canada (NSERC) under a Strategic Research Grant.

C. Tellambura is with the Department of Digital Systems, Monash University, Clayton, Victoria 3168, Australia (e-mail: chintha@dgs.monash.edu.au).

A. J. Mueller is with Digital Dispatch Systems, Inc., Richmond, B.C., Canada.

V. K. Bhargava is with the Department of Electrical and Computer Engineering University of Victoria, Victoria, B.C., Canada V8W 3P6.

Publisher Item Identifier S 0018-9545(97)04626-4.

average BER, $E\{g(\exp(-kS))\}$. A straightforward method is to find the probability density function (pdf) of S and then to evaluate the average BER. Instead, supposing we have the MGF of S given by $m(z) = E\{\exp(-zS)\}$, we then find that the average BER can be readily expressed in terms of $m(k)$. This approach naturally lends itself useful to cases, where the MGF is readily available, such as diversity reception with MRC. We should also observe that some results (e.g., in [5]) in the literature can be readily derived with this approach. Second, extensive use is made of classical numerical integration techniques, namely Gauss–Hermite and Gauss–Laguerre methods. Such techniques have previously been limited to the study of cochannel interference problems [3]. Also included are some results concerning their accuracy when applied to cases of shadowing.

This paper is organized as follows. In Section II, the required statistical properties of the channel model proposed in [1] are derived. These statistical properties are extended for the channel with microdiversity combining in Section III. In Section IV, the average BER is determined as a function of the channel statistics for M-PSK and M-DPSK ($M \geq 2$), and in Section V, the outage probability is determined. Using the channel parameters measured in [1], the results of our numerical evaluation are presented in Section VI. Finally, in Section VII we summarize our conclusions.

II. Channel Model Statistics

In the following analysis, the MGF and the cumulative distribution function (CDF) for the received power over a single fading channel are derived. Making the slow fading assumption (i.e., the channel is slowly varying with respect to $1/T$, where T is the symbol duration), the received signal corresponding to the kth transmitted symbol may be expressed as

$$y_k = s_k x_k + n_k \tag{1}$$

where x_k is the transmitted signal corresponding to the k th information symbol, n_k is additive Gaussian noise with a single-sided spectral density $N_0/2$, and s_k is the complex channel gain (equal to unity in the absence of fading). In complex notation, $s_k = s_{k,I} + j s_{k,Q}$, where $s_{k,I}$ and $s_{k,Q}$ are the in-phase and quadrature components of the fading envelope, respectively. The received power in the faded envelope is then $S = |s|^2 = s_I^2 + s_Q^2$ (where k is omitted for notational ease). The signal-to-noise ratio (SNR) γ in the unfaded link is then defined as

$$\gamma = E[|x_k|^2]/N_0 = E_s/N_0. \tag{2}$$

In [1] and [2], a two-state channel model based on channel measurements is presented (Fig. 1). For a fraction of the time $1 - A$, the channel is in the good state modeled as a Rician random process. For the remaining fraction of the time A, the channel is in the bad state modeled as a lognormally shadowed Rayleigh random process, or equivalently, a Suzuki random process. The net pdf of the received power is thus the weighted sum of the Rician and Suzuki pdf's $p_{\text{Rice}}(S)$ and $p_{\text{Suzuki}}(S)$,

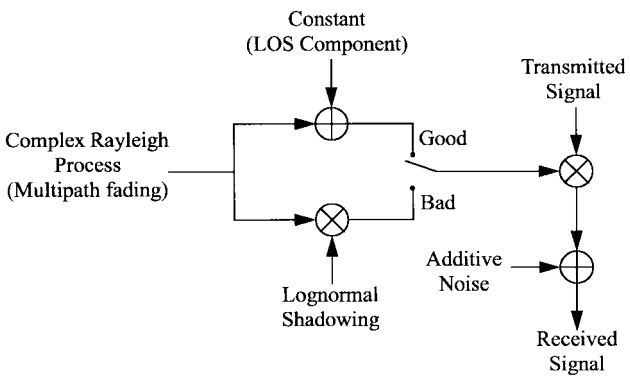

Fig. 1. Functional diagram of the channel model.

respectively,

$$p(S) = (1 - A)p_{\text{Rice}}(S) + A p_{\text{Suzuki}}(S). \tag{3}$$

Similarly, using the definition of the MGF [7], the net MGF for the channel is

$$m(z) = \int_0^\infty e^{-zS} p(S)\, dS = (1-A)m_{\text{Rice}}(z) + A m_{\text{Suzuki}}(z) \tag{4}$$

where $m_{\text{Rice}}(z)$ and $m_{\text{Suzuki}}(z)$ are the MGF's for the Rician and Suzuki fading states, respectively. Finally, by integrating (3), the net cumulative distribution (CDF) with respect to the Rician and Suzuki CDF's, $F_{\text{Rice}}(S)$ and $F_{\text{Suzuki}}(S)$, is obtained

$$F(S) = \int_0^S p(x)\, dx = (1-A)F_{\text{Rice}}(S) + A F_{\text{Suzuki}}(S). \tag{5}$$

A. Rician Channel

Rician fading characterizes channels, where a direct LOS path exists between the transmitter and receiver, as well as a multipath component comprising multiple scattered and reflected paths. For Rician fading, s_I and s_Q are independent Gaussian random processes, where s_I has a mean equal to the signal strength in the LOS path, s_Q has zero mean and both have the same variance equal to the power in the multipath component [7]. The received faded power therefore obeys the noncentral Chi-squared distribution with two degrees of freedom. Since the expressions for the CDF and MGF for the Chi-squared distribution are well known (see [7]), they are repeated here without explanation. The CDF is given as

$$F_{\text{Rice}}(S) = 1 - Q(\sqrt{2K}, \sqrt{2(1+K)S}) \tag{6}$$

where K is the Rice factor defined as the ratio of the power in the LOS path to the power in the diffuse paths and $Q(\alpha, \beta)$ is Marcum's Q function (see [9, Appendix C]). Note that (6) is obtained by setting the expected value of the power to unity. Similarly, the MGF is given as

$$m_{\text{Rice}}(z) = \frac{1+K}{1+K+z} e^{-\left[\frac{zK}{1+K+z}\right]}. \tag{7}$$

When an LOS path does not exist, K approaches zero and (6) and (7) default to the *normalized* Rayleigh fading case as expected.

B. Suzuki Channel

Suzuki fading characterizes the joint effects of Rayleigh fading and lognormal shadowing and models a shadowed multipath channel without an LOS path. Over a local area, the fading envelope obeys a Rayleigh distribution with a local area mean power S_0. Due to changing topographical features, S_0 varies over larger areas following a lognormal distribution. The MGF of the Suzuki faded received power is therefore defined as

$$m_{\text{Suzuki}}(z) = \int_0^\infty \int_0^\infty e^{-zS} p_{\text{Rayl}}(S|S_0) p_{\ln}(S_0)\, dS_0\, dS. \tag{8}$$

The integration with respect to S is the MGF of the Rayleigh faded signal power. Since for Rayleigh fading, s_I and s_Q are independent zero-mean Gaussian random processes with variance equal to the power of the multipath component [7], the received faded power obeys the central Chi-squared distribution with two degrees of freedom. Therefore, the MGF for a mean power S_0 is [7]

$$m_{\text{Rayl}}(z) = \frac{1}{1+zS_0}. \tag{9}$$

Substituting (9) and $p_{\ln}(S_0)$ as given in [3] into (8), we get

$$m_{\text{Suzuki}}(z) = \int_0^\infty \frac{\exp\left[-\ln^2\left(\frac{S_0}{\mu}\right)/(2\sigma^2)\right]}{\sqrt{2\pi}\sigma S_0(1+zS_0)}\, dS_0 \tag{10}$$

where σ is the logarithmic standard deviation in natural units and μ is the local mean power. Using the variable substitution $x = \ln(S_0/\mu)/(\sqrt{2}\sigma)$ presented in [3] and applying Hermitian integration [8], we get an exact closed-form expression for the Suzuki MGF

$$m_{\text{Suzuki}}(z) = \frac{1}{\sqrt{\pi}} \sum_{i=1}^{n} \frac{w_i}{1+za_i} + R_n \tag{11}$$

where a_i is equal to $\mu \exp(\sqrt{2}\sigma x_i)$, x_i and w_i are the ith abscissa and weight, respectively, of the nth-order Hermite polynomial (tabulated in [8]), and R_n is a remainder term. An upper bound on the remainder term is derived in Appendix I. For $\sigma < 4.3$ dB, the error term is negligible. However, for larger σ, R_n is still negligible, but this fact cannot be established by means of the upper bound. In this case, Simpson's integration (Appendix II) can be used to verify the accuracy of the Hermitian integration.

Since the pdf and MGF are a Laplace transform pair, the Suzuki pdf can be readily obtained by finding the inverse Laplace transform of (11). Integrating the resulting pdf, the Suzuki CDF is found to be

$$F_{\text{Suzuki}}(S) = \frac{1}{\sqrt{\pi}} \sum_{i=1}^{n} w_i[1 - e^{-S/a_i}] + R_n. \tag{12}$$

III. Diversity Reception

Diversity reception is employed to mitigate the effects of short-term fading. The underlying premise is that if two or more signals are taken from "sufficiently" spaced receiving antennas, then it is improbable that these signals will experience simultaneous deep fades. Diversity reception can be used either at the base station or at the mobile, although the antenna separation required differs in each case. For instance, when diversity is employed at the mobile (referred to as microdiversity), an antenna separation of $0.5\,\lambda$ has been found to achieve almost independently fading diversity branches. Macrodiversity, which is not covered in this paper, implies the combining of signals from multiple base stations. In practice then, microdiversity reception can combat the rapid variations in the received signal strength caused by multipath fading. To capitalize on this improvement in signal statistics, several combining methods have been proposed. We consider selection diversity combining (SDC) and maximal ratio combining (MRC) and derive the new CDF's and MGF's for the power in the received envelope after combining. Due to the larger area effect of shadowing and the limited antenna separation distance at the mobile, antenna separation cannot decorrelate the effects of shadowing between antennas. In fact, it is assumed that the shadowing effects at each antenna are identical.

A. SDC

Perhaps the simplest combining method, SDC, measures the SNR at each branch (i.e., antenna) and selects the branch with the highest SNR value. If L-branch diversity is employed and the mean noise power per branch is the same for all branches, the decision criteria reduce to $\max S_i,\ i = 1, \cdots, L$, where S_i is the power from the ith branch. The probability that $S_i,\ i = 1, \cdots, L$ are all simultaneously less than or equal to some S is $\prod_i \Pr(S_i \le S)$. Since for the multipath channel, $S_i,\ i = 1, \cdots, L$ are uncorrelated and identically distributed, this probability is equal to the CDF for the power in one branch raised to the power L.

For the Rician channel, the CDF for the power in one branch is given by (6). Therefore, the CDF for the Rician channel with L-branch diversity is

$$F_{\text{Rice}}^{(\text{SDC})}(S) = \left[1 - Q(\sqrt{2K}, \sqrt{2(1+K)S}\right]^L. \tag{13}$$

Performing the Laplace transform on the derivative of (13) results in the corresponding MGF. Therefore, using the Laplace transform of a derivative property [8] and expressing the Laplace transform as an integral, the MGF becomes

$$m_{\text{Rice}}^{(\text{SDC})}(z) = z \int_0^\infty e^{-zS}\left[1 - Q(\sqrt{2K}, \sqrt{2(1+K)S}\right]^L dS. \tag{14}$$

By making the variable substitution $x = zS$ and applying the Gauss–Laguerre integration approximation [8], the expression for the MGF becomes

$$m_{\text{Rice}}^{(\text{SDC})}(z) \approx \sum_{i=1}^{n} \omega_i\left[1 - Q(\sqrt{2K}, \sqrt{2(1+K)\chi_i/z}\right]^L \tag{15}$$

where ω_i and χ_i are the i th abscissa and weight, respectively, of the nth-order Laguerre polynomial (tabulated in [8]). As $n \to \infty$, (15) approaches equality (Appendix I).

For the Suzuki channel state, consider first the uncorrelated Rayleigh components conditioned on S_0. For L-branch SDC diversity, the Rayleigh CDF is equal to the nondiversity CDF

[7] raised to the power L

$$F_{\text{Rayl}}^{(\text{SDC})}(S|S_0) = (1 - e^{-S/S_0})^L. \tag{16}$$

Applying the binomial expansion to (16) and performing the Laplace transform (using the Laplace transform of a derivative property), the Rayleigh MGF conditioned on S_0 for SDC is

$$m_{\text{Rayl}}^{(\text{SDC})}(z) = \sum_{j=0}^{L} (-1)^j \binom{L}{j} \frac{zS_0}{j + zS_0}. \tag{17}$$

Following the same procedure as used to obtain (11), the MGF for the Suzuki channel with SDC can be easily found

$$m_{\text{Suzuki}}^{(\text{SDC})}(z) = \frac{1}{\sqrt{\pi}} \sum_{i=1}^{n} w_i \sum_{j=0}^{L} (-1)^j \binom{L}{j} \frac{za_i}{j + za_i} + R_n \tag{18}$$

where a_i, w_i, and R_n were defined for (11). The corresponding Suzuki CDF can be obtained by performing the inverse Laplace transform on (18) to get the pdf and integrating. However, since the summation over j in (18) is equal to the MGF given in (17), where a_i replaces S_0, the CDF for the Suzuki channel can be written directly from (16)

$$F_{\text{Suzuki}}^{(\text{SDC})}(S) = \frac{1}{\sqrt{\pi}} \sum_{i=1}^{n} w_i (1 - e^{-S/a_i})^L + R_n. \tag{19}$$

As expected, (13), (18), and (19) revert to the nondiversity case when $L = 1$. Since a closed-form expression for (15) exists for the nondiversity case, (15) does not directly revert to (7) when $L = 1$. Previously, just one paper [13] appears to have analyzed this case, using a different formula.

B. MRC

Of any known linear diversity combiner, MRC provides the best statistical reduction of multipath fading [10]. Rather than selecting one signal as in SDC, each signal is weighted proportionately to their SNR and then summed. It is shown in [10] that for L-branch diversity, the total signal power S is the sum of the received signal power S_i, $i = 1, \cdots, L$ from each antenna.

For the Rician channel, the CDF and MGF are obtained easily by recognizing that S is now distributed as a noncentral Chi-squared random process with $2L$ degrees of freedom. From [7], the CDF is

$$F_{\text{Rice}}^{(\text{MRC})}(S) = 1 - Q_L(\sqrt{2LK}, \sqrt{2(1+K)S}) \tag{20}$$

where $Q_m(\alpha, \beta)$ is the generalized Marcum's Q function. Note that K is defined as before, but now the expected value of S is L (i.e., each branch is normalized). Similarly, the MGF for S is [7]

$$m_{\text{Rice}}^{(\text{MRC})}(z) = \left(\frac{1+K}{1+K+z}\right)^L e^{-\left[\frac{zKL}{1+K+z}\right]}. \tag{21}$$

As expected for the sum of uncorrelated and identically distributed random variables, the MGF of S with diversity is simply the MGF of S without diversity raised to the power L.

For the Suzuki channel, the Rayleigh fading components are uncorrelated between antennas, but have a common local area mean S_0, which is lognormally distributed. The corresponding closed-form MGF can be obtained following the same procedure used to obtain (11). However, since S conditioned on S_0 can be considered the sum of uncorrelated and identically distributed S_i, $i = 1, \cdots, L$ also conditioned on S_0, the MGF of the Rayleigh fading is equal to that in (9) raised to the power L. Thus, the Suzuki MGF for MRC diversity is

$$m_{\text{Suzuki}}^{(\text{MRC})}(z) = \frac{1}{\sqrt{\pi}} \sum_{i=1}^{n} \left[\frac{w_i}{1 + za_i}\right]^L + R_n. \tag{22}$$

Finding the inverse Laplace transform of (22) to obtain the pdf and integrating, the CDF is found to be

$$F_{\text{Suzuki}}^{(\text{MRC})}(S) = \frac{1}{\sqrt{\pi}} \sum_{i=1}^{n} w_i \left[1 - e^{-S/a_i} \sum_{m=0}^{L-1} \frac{(S/a_i)^m}{m!}\right] + R_n. \tag{23}$$

Note that (20)–(23) default back to the nondiversity case when $L = 1$ as expected.

IV. Average BER

In this section, expressions for the average BER for coherent M-ary PSK and M-ary DPSK are derived. The average BER is defined as the number of erroneous bits per block of transmitted bits averaged over all time to account for all channel fading variations. Thus, we are interested in the expected value of the BER given by the integral over the range $0 < S < \infty$

$$\overline{P}_{\text{b}}(\gamma) = \int_0^\infty P_b(\gamma|S) p(S)\, dS \tag{24}$$

where γ is the SNR for the unfaded link given in (2), S is the instantaneous signal power, $P_b(\gamma|S)$ is the instantaneous BER conditioned on S, and $p(S)$ is the pdf of the fading channel power. By expressing (24) in terms of the received power's MGF, the BER expressions can be written independent of the type of fading or diversity employed.

A. Binary PSK and DPSK

For $M = 2$, M-ary PSK and DPSK revert to the more common binary case. As a simple expression for the binary case exists, it is considered separately from the more general M-ary case. For binary PSK, the instantaneous BER is [7]

$$P_{\text{b}}^{(\text{PSK})}(\gamma|S) = \frac{1}{2}\text{erfc}(\sqrt{S\gamma}) \tag{25}$$

where $\text{erfc}(x)$ is the complementary error function. An alternate exponential form for $\text{erfc}(x)$ can be obtained by rearranging [8, (7.4.11)] by substituting $t = x \tan\theta$

$$\text{erfc}(x) = \frac{2}{\pi} \int_0^{\pi/2} e^{-x^2 \sec^2\theta}\, d\theta. \tag{26}$$

This form is both easily evaluated and well suited to numerical integration since the integrand is well behaved over the range of the integral. Substituting this alternative form into (25), the average BER in (25) can be written as

$$\overline{P}_{\text{b}}^{(\text{PSK})}(\gamma) = \frac{1}{\pi} \int_0^\infty \int_0^{\pi/2} e^{-S\gamma \sec^2\theta} p(S)\, d\theta\, dS. \tag{27}$$

By interchanging the order of integration and recognizing that the integral with respect to S is equal to the MGF of the fading channel evaluated at $\gamma \sec^2\theta$, (27) can be rewritten in the desired form

$$\overline{P}_{\mathrm{b}}^{(\mathrm{PSK})}(\gamma) = \frac{1}{\pi}\int_0^{\pi/2} m[\gamma \sec^2\theta]\, d\theta. \tag{28}$$

In general, a closed-form expression for (28) cannot be obtained. However, if the channel's MGF is of the form $m(z) = (1+za)^{-L}$, one can directly solve (24) for the BPSK case [7, (7.4.15)]

$$\overline{P}_{\mathrm{b}}(\gamma) = \phi(a\gamma, L) \tag{29}$$

where we define $(x \geq 0)$ $\tilde{x} = \sqrt{x/(1+x)}$ and

$$\phi(x,L) = \left(\frac{1-\tilde{x}}{2}\right)^L \sum_{k=0}^{L-1}\binom{L-1+k}{k}\left(\frac{1+\tilde{x}}{2}\right)^k. \tag{30}$$

For the SDC, Rician channel case, (15) is not of the correct form and the average BER must be determined from (28). For the SDC, Suzuki channel case, (18) can be easily manipulated into the desired form to obtain (ignoring R_n)

$$\overline{P}_{\mathrm{b,Suzuki}}^{(\mathrm{SDC,BPSK})}(\gamma) = \sum_{i=1}^{n}\frac{w_i}{\sqrt{\pi}}\sum_{j=0}^{L}(-1)^j\binom{L}{j}[1-\phi(a_i/j,1)] \tag{31}$$

where w_i and a_i are given for (11). Using the series expansion for the exponential term, the MGF for the MRC, Rician channel (21) can be written in the desired form

$$m_{\mathrm{Rice}}^{(\mathrm{MRC})}(z) = e^{-KL}\sum_{n=0}^{\infty}\frac{(KL)^n}{n!(1+az)^{n+L}} \tag{32}$$

where $a = (1+K)^{-1}$. Thus, the closed-form expression for the average BER is

$$\overline{P}_{\mathrm{b,Rice}}^{(\mathrm{MRC,BPSK})}(\gamma) = e^{-KL}\sum_{n=0}^{\infty}\frac{(KL)^n}{n!}\phi(a\gamma, n+L) \tag{33}$$

which is a rapidly converging series.[1] Note, when $K = 0$, (33) resorts to the Rayleigh fading case [7]. In fact, Lindsey [12] derives an alternate expression for (33). This is a recursion formula containing a confluent hypergeometric function. Thus, (33) is much easier to compute.

Finally, since the MGF for the MRC Suzuki channel (22) is already in the desired form, the average BER is (ignoring R_n)

$$\overline{P}_{\mathrm{b,Suzuki}}^{(\mathrm{MRC,BPSK})}(\gamma) = \frac{1}{\sqrt{\pi}}\sum_{i=1}^{n} w_i\phi(a_i, L). \tag{34}$$

For binary DPSK, the instantaneous BER is [7]

$$P_{\mathrm{b}}^{(\mathrm{DPSK})}(\gamma) = \frac{1}{2}e^{-S\gamma}. \tag{35}$$

[1]The following recursive property can be exploited in the computation of (33):

$$\phi(x, L+1) = \phi(x,L) - \sqrt{\frac{x}{1+x}}\left(\frac{1}{4(1+x)}\right)^L\binom{2L-1}{L}.$$

Substituting (35) into (24) and interchanging the order of integration, the average BER can be written in terms of the MGF

$$\overline{P}_{\mathrm{b}}^{(\mathrm{DPSK})}(\gamma) = \frac{1}{2}m(\gamma). \tag{36}$$

B. M-ary PSK and DPSK $(M > 2)$

Coherent M-PSK maps each block of $k = \log_2 M$ bits to one of unique symbols each separated by a phase offset equal to $2\pi/M$. Demodulation is performed by measuring the phase offset between the received signal and some fixed reference. When the received signal is perturbed by an instantaneous SNR equal to $S\gamma$, the CDF of the phase error θ is [11], [5]

$$\begin{aligned} F_{\mathrm{PSK}}(\psi,\gamma|S) &= \Pr[-\pi < \theta < \psi], \qquad -\pi < \psi < 0 \\ &= \frac{1}{2\pi}\int_{-\pi/2}^{\pi/2+\psi} e^{-S\gamma\sin^2\psi\sec^2\theta}\, d\theta \end{aligned} \tag{37}$$

where S is the fading channel gain and γ is the SNR for the unfaded link. Averaging (37) over the pdf of the fading channel $p(S)$ and interchanging the order of integration, the average CDF of the phase error as a function of the channel MGF can be obtained

$$F_{\mathrm{PSK}}(\psi,\gamma) = \frac{1}{2\pi}\int_{-\pi/2}^{\pi/2+\psi} m[\gamma\sin^2\psi\sec^2\theta]\, d\theta. \tag{38}$$

With the possible exception of some channel types, a closed-form expression for (38) is difficult or impossible to obtain. It is, however, well suited for numerical integration.

For noncoherent M-DPSK, the difference between adjacent M-ary symbols is mapped to one of unique symbols. Demodulation is performed by measuring the phase offset between adjacent received symbols. For an instantaneous SNR equal to $S\gamma$, the CDF of the phase error between the two received signals is [5], [11]

$$\begin{aligned} &F_{\mathrm{DPSK}}(\psi,\gamma|S) \\ &\quad = \frac{-\sin\psi}{4\pi}\int_{-\pi/2}^{\pi/2}\frac{\exp[-S\gamma(1-\cos\psi\cos t)]}{1-\cos\psi\cos t}\, dt. \end{aligned} \tag{39}$$

Averaging (39) over $p(S)$ and interchanging the integration order, the average CDF of θ in terms of the channel's MGF is

$$F_{\mathrm{DPSK}}(\psi,\gamma) = \frac{-\sin\psi}{4\pi}\int_{-\pi/2}^{\pi/2}\frac{m[\gamma(1-\cos\psi\cos t)]}{1-\cos\psi\cos t}\, dt. \tag{40}$$

Again, for most channel models, a closed-form expression of (40) is difficult or impossible to obtain, however, it is well suited to numerical integration.

When demodulating M-PSK and M-DPSK, if the jth symbol was transmitted, the $(i+j)$th symbol is demodulated if θ falls within the range $-(2i+1)\pi/M$ and$-(2i-1)\pi/M$. The corresponding BER is the Hamming distance between the ith and jth symbols divided by the number of bits per symbol. Assuming all symbols are transmitted with equal probability, the average BER is

$$\overline{P}_{\mathrm{b}}(\gamma) = \frac{2}{\log_2 M}\sum_{i=1}^{M/2} d_i^{(M)}\Pr[-\theta_i < \theta \leq -\theta_{i-1}] \tag{41}$$

TABLE I
AVERAGE HAMMING DISTANCE BETWEEN SYMBOLS FOR GREY CODE

M	$d_i^{(M)}, i = 1, 2, \ldots, M/2$
4	$1, 2$
8	$1, 2, 2, 2$
16	$1, 2, 2, 2, \frac{5}{2}, 3, \frac{5}{2}, 2$
32	$1, 2, 2, 2, \frac{5}{2}, 3, \frac{5}{2}, 2, \frac{11}{4}, \frac{7}{2}, \frac{13}{4}, 3, \frac{13}{4}, \frac{7}{2}, \frac{11}{4}, 2$
64	$1, 2, 2, 2, \frac{5}{6}, 3, \frac{5}{2}, 2, \frac{11}{4}, \frac{7}{2}, \frac{13}{4}, 3, \frac{13}{4}, \frac{7}{2}, \frac{11}{4}, 2,$ $\frac{23}{8}, \frac{15}{4}, \frac{29}{8}, \frac{7}{2}, \frac{31}{8}, \frac{17}{4}, \frac{29}{8}, 3, \frac{29}{8}, \frac{17}{4}, \frac{31}{8}, \frac{7}{2}, \frac{29}{8}, \frac{15}{4}, \frac{23}{8}, 2$

where $\theta_i \triangleq (2i+1)\pi/M$ for $i = 1, \cdots, M/2-1$, $\theta_{M/2} \triangleq \pi$, and $d_i^{(M)}$ is the Hamming distance between the ith and jth symbols averaged over all j. Assuming Grey code symbol mapping, the average Hamming distance can be found through simple iteration through all i and j averaged over j. Table I lists $d_i^{(M)}$ for symbol sizes of 2–5 b long. From the definition of the CDF, the following property is evident:

$$\Pr[\psi_1 < \theta \leq \psi_2] = F(\psi_2) - F(\psi_1).$$

Applying this to (41) we get the desired expression for the average BER

$$\overline{P}_{\rm b}(\gamma) = \frac{2}{\log_2 M} \sum_{i=1}^{M/2} d_i^{(M)} [F(-\theta_{i-1}, \gamma) - F(-\theta_i, \gamma)] \quad (42)$$

where $F(\psi, \gamma)$ is given by (38) for M-PSK and by (40) for M-DPSK.

V. OUTAGE PROBABILITY

Often, a more useful measure of transmission quality, the outage probability $P_{\rm out}$, indicates the percentage of the time that the instantaneous BER is above some acceptable threshold, ϵ. For voice data, the threshold can be as high as 10^{-2} to ensure toll-quality speech. For data (uncoded) transmission, the threshold is about 10^{-4}. For video data, BER requirements can be even more stringent. Since the instantaneous BER $P_b(S)$ is a monotonically decreasing function of S, $P_{\rm out}$ can be written as

$$P_{\rm out} = \Pr[S < \hat{S}] = F(\hat{S}] \quad (43)$$

where $\hat{S}$ is the solution to $P_b(S) = \epsilon$ and $F(S)$ is the CDF of the fading channel. Thus, given $\hat{S}$, the outage probability can be expressed in terms of the channel's CDF independent of channel type or diversity scheme employed.

A. Binary PSK and DPSK

Compared to the M-ary $(M > 2)$ case, the outage probability for binary PSK and DPSK is easily derived. For PSK, $\hat{S}$ is obtained by rearranging (25) to get

$$\hat{S} = \frac{1}{\gamma}[\text{erfc}^{-1}(2\epsilon)]^2 \quad (44)$$

where approximations to the inverse erfc function can be found in many mathematical references (see [8]). The outage probability is obtained by substituting $\hat{S}$ from (44) into (43). For DPSK, $\hat{S}$ is obtained by rearranging (35) to get

$$\hat{S} = -\frac{\ln(2\epsilon)}{\gamma}. \quad (45)$$

Substituting $\hat{S}$ from (45) into (43) results in the outage probability for DPSK.

B. M-ary PSK and DPSK $(M > 2)$

For both M-ary PSK and DPSK, no easy method for obtaining $\hat{S}$ exists. For both M-PSK and M-DPSK, $\hat{S}$ is the solution to

$$\frac{2}{\log_2 M} \sum_{i=1}^{M/2} d_i^{(M)} [F(-\theta_{i-1}, \gamma) - F(-\theta_i, \gamma)] = \epsilon \quad (46)$$

where $F(\psi, \gamma)$ for M-PSK is given by (37) with $\hat{S}$ replacing S and $F(\psi, \gamma)$ for M -DPSK is given by (39), where, again, $\hat{S}$ replaces S. Since the BER is monotonically decreasing, the solution to (46) is not too difficult to find. Once $\hat{S}$ is found, the outage probability can be obtained directly from (43).

VI. NUMERICAL RESULTS

Numerical results are presented for the average BER and outage probability. The results are based on a per-branch E_b/N_0 (i.e., on average, MRC with L branches has L times more signal energy than a single channel). Where Hermitian or Laguerre approximations to integration are performed, orders of 20 and 15, respectively, are used. For other integrations, a routine, which successively doubles the number of integration points, is used to obtain a relative accuracy greater than 10^{-6}. When finding the solution to (46), the bisection root-finding method is employed to obtain $\hat{S}$ with a relative accuracy of 10^{-6}.

TABLE II
PARAMETER SETS FOR THE ANALOG CHANNEL MODEL [1]

Parameter set	A	K, dB	μ, dB	σ, dB
Munich city (24°)	0.70	8.7	-8.5	3.0
Munich wood (24°)	0.54	10.7	-5.3	1.3
Munich highway (24°)	0.16	11.7	-7.0	4.5
Hamburg city (21°)	0.75	9.4	-8.7	3.2
Copenhagen city (18°)	0.80	5.5	-9.4	3.0
Stockholm city (13°)	0.87	7.0	-9.5	3.0

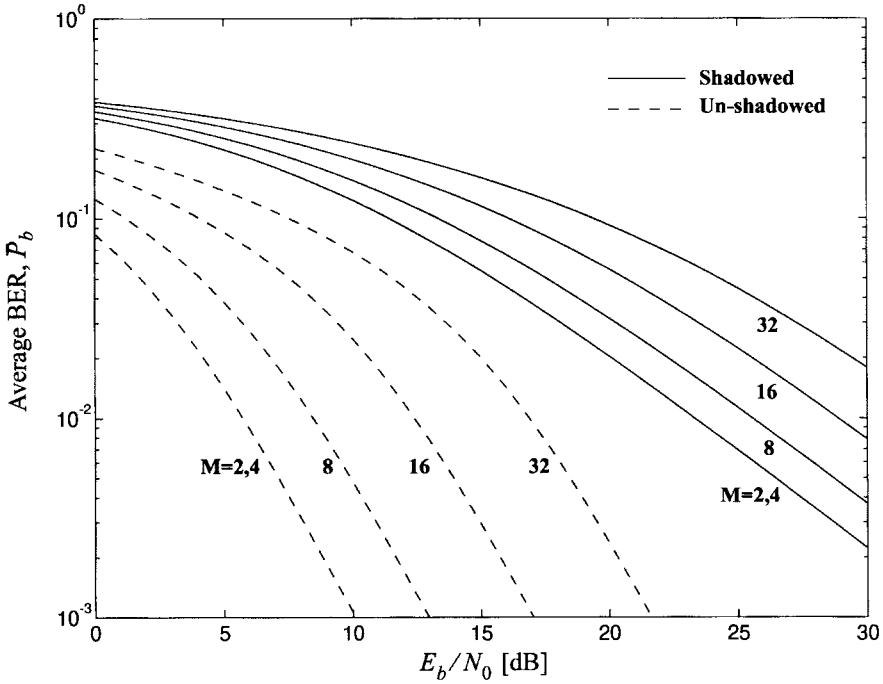

Fig. 2. Average BER of M-ary PSK ($M = \{2, 4, 8, 16, 32\}$) in the shadowed and unshadowed Munich city environment.

The parameters used to represent the fading channel are taken from [1]. These are repeated in Table II. Note that conversions from decibels to linear units is required for K and μ, and conversion from decibels to nepers for σ. The angle immediately following the location specifies the elevation angle between the earth and geostationary satellite for which the measurements were performed.

A. Average BER

Fig. 2 illustrates the average BER of M-ary PSK for $M = \{2, 4, 8, 16, 32\}$ in the shadowed and unshadowed Munich city environment. At an average BER of 10^{-2}, typical of voice communications, the performance when shadowed (i.e., $A = 1$) is about 16 dB worse than when unshadowed ($A = 0$). Furthermore, increasing the symbol size beyond two bits (i.e., $M = 4$) degrades the BER performance from 2 to 4 dB. To achieve an average BER of 10^{-2}, an SNR of 6.3, 9.0, 13.0, and 17.4 dB in the unshadowed environment and an SNR of 23.8, 25.5, 29., 32.8 dB in the shadowed environment is required for $M = \{4, 8, 16, 32\}$, respectively. As expected, the performance of DPSK (not shown) was found to be worse than that of PSK. Thus, to achieve a desired BER at a reasonable SNR, some method of improving the performance is required. Microdiversity is one such method.

For M-ary PSK, the improvement in BER when MRC microdiversity is employed is shown in Fig. 3 for the Munich city environment. Note the significant improvement in BER due to microdiversity. For example, at a BER of 10^{-2}, an SNR gain of 7.1 and 13.1 dB can be achieved using $L = \{2, 5\}$ branch MRC diversity over no diversity (relatively independent of M). Note that the penalty for increasing the constellation size above that of BPSK or QPSK is about 2.3 and 5.8 dB (relatively independent of L) for $M = \{8, 16\}$. Thus, by employing two-branch MRC, the BER performance of 16-ary PSK surpasses that of BPSK or QPSK without diversity.

Fig. 4 shows the average BER for differentially detected QPSK (i.e., $M = 4$) with both MRC and SDC microdiversity in the Munich city fading environment. Comparing the diversity cases to the nondiversity case, we see that a significant increase in BER performance can be achieved

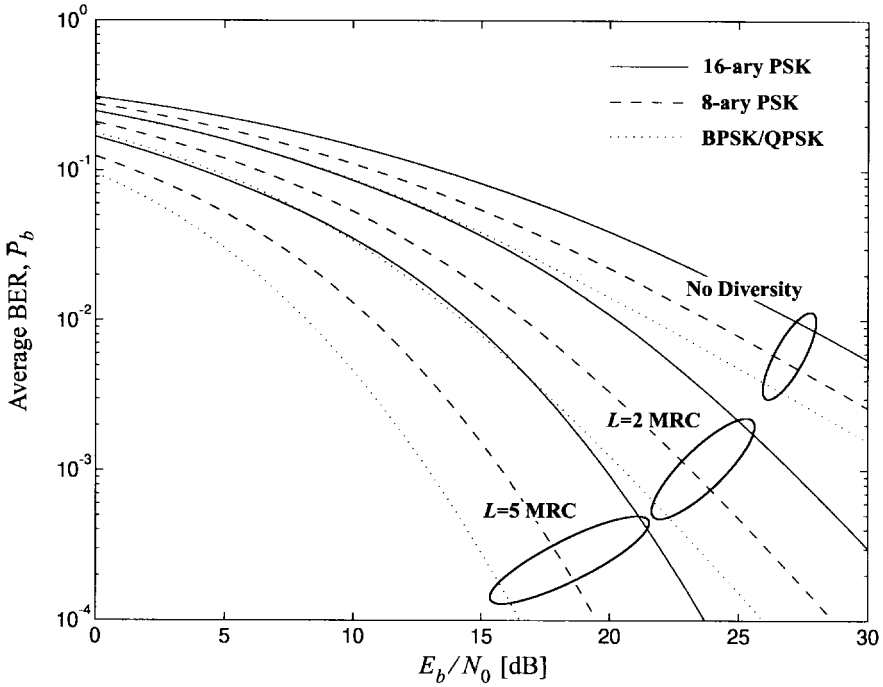

Fig. 3. Average BER of M-ary PSK ($M = \{2, 4, 8, 16\}$) with MRC microdiversity ($L = \{1, 2, 5\}$) in the Munich city environment.

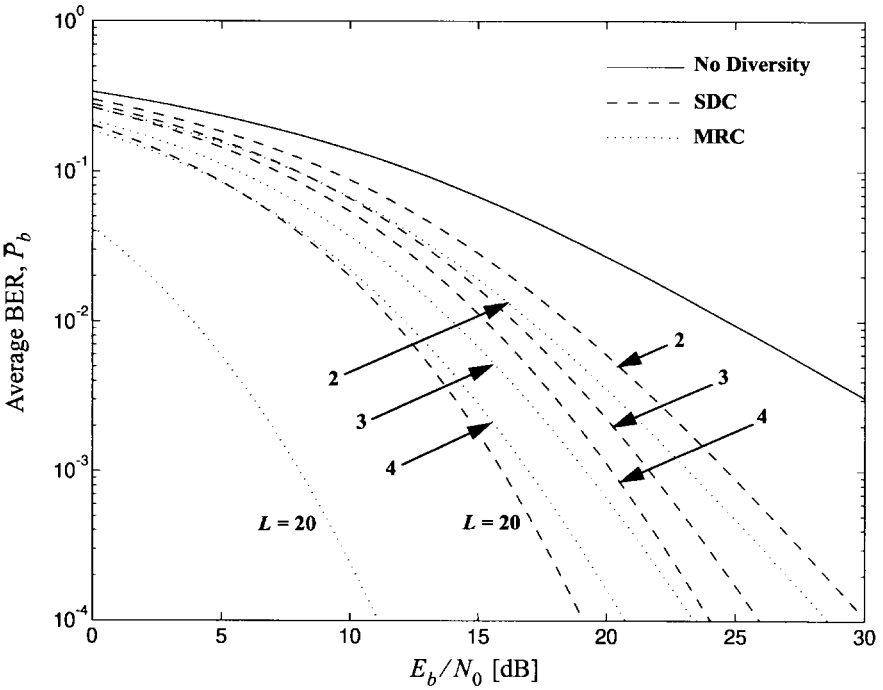

Fig. 4. Average BER of four M-ary DPSK (differential QPSK) with L-branch microdiversity in the Munich city environment.

through diversity, particularly for MRC. For an average BER of 10^{-2}, an SNR improvement of 6.2, 8.3, and 9.4 dB for SDC and 7.6, 10.7, and 12.5 dB for MRC can be achieved over the nondiversity case for $L = \{2, 3, 4\}$, respectively. Note that as the number of branches increases, the incremental savings in SNR decreases. The BER curves for $L = 20$ illustrates this and further emphasizes the advantage of MRC over SDC.

The average BER for binary DPSK with MRC diversity for two and three branches is shown in Fig. 5 for the city and highway environment around Munich. Of interest is the declining dependence on the fading environment as the diversity order increases. At a BER of 10^{-2}, the difference in SNR between the city and highway environments is 7.8, 5.5, and 4.8 dB for $L = \{1, 2, 3\}$, respectively. This effect is even more pronounced at a BER of 10^{-4}, where the difference in

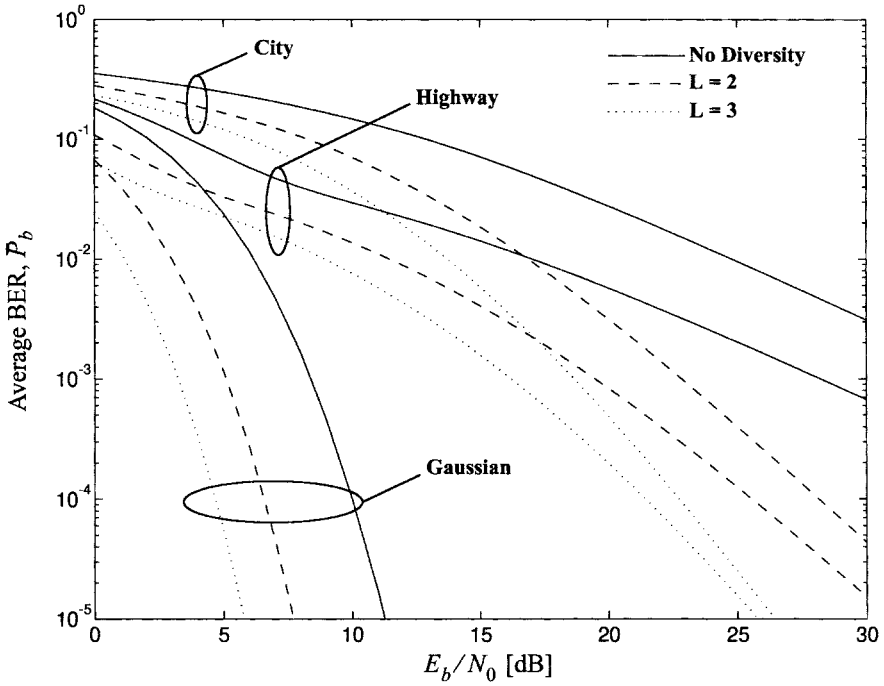

Fig. 5. Average BER of binary DPSK with and without microdiversity in the city and highway environments around Munich. Performance of the Gaussian channel is provided for comparison.

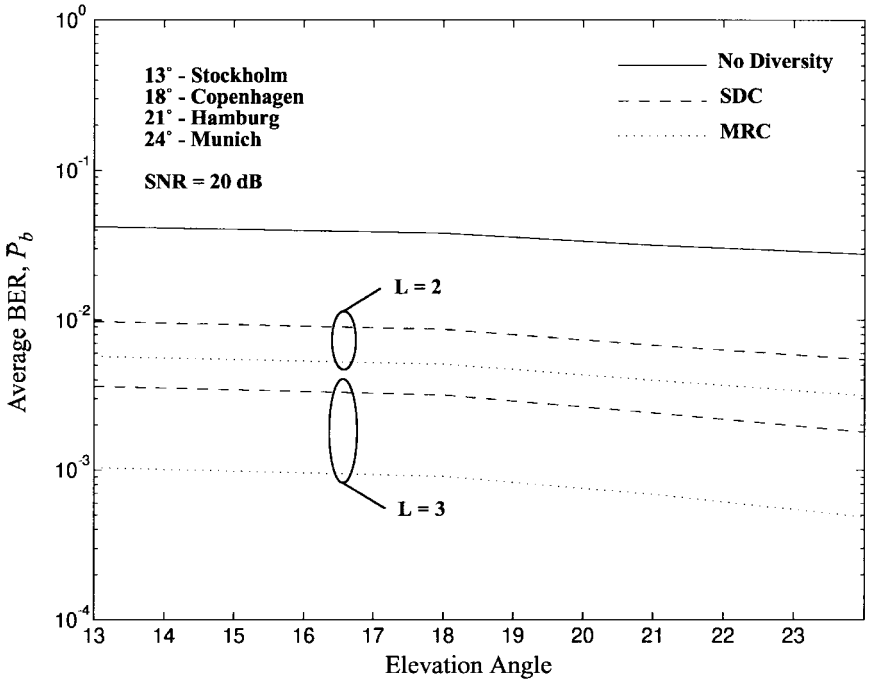

Fig. 6. Average BER of binary DPSK with microdiversity in the city environment as a function of the elevation angle for a fixed SNR of 20 dB.

SNR between the two environments is 6.7, 2.6, and 1.3 dB for $L = \{1, 2, 3\}$. For satellite systems, where a single transmitter serves multiple environments, increasing the diversity order will reduce the excess signal power when the mobile is in a favorable environment.

Finally, Fig. 6 illustrates the average BER for DPSK with diversity in the city environment as a function of the elevation angle for an SNR of 20 dB. As anticipated, the BER decreases as the elevation angle increases due to the decrease in shadowing effects. Although improving the BER performance, the diversity techniques do not mitigate the elevation angle effects. This is anticipated since the elevation angle affects primarily the degree of shadowing, which cannot be combatted with microdiversity techniques. The shallow slope of the curves

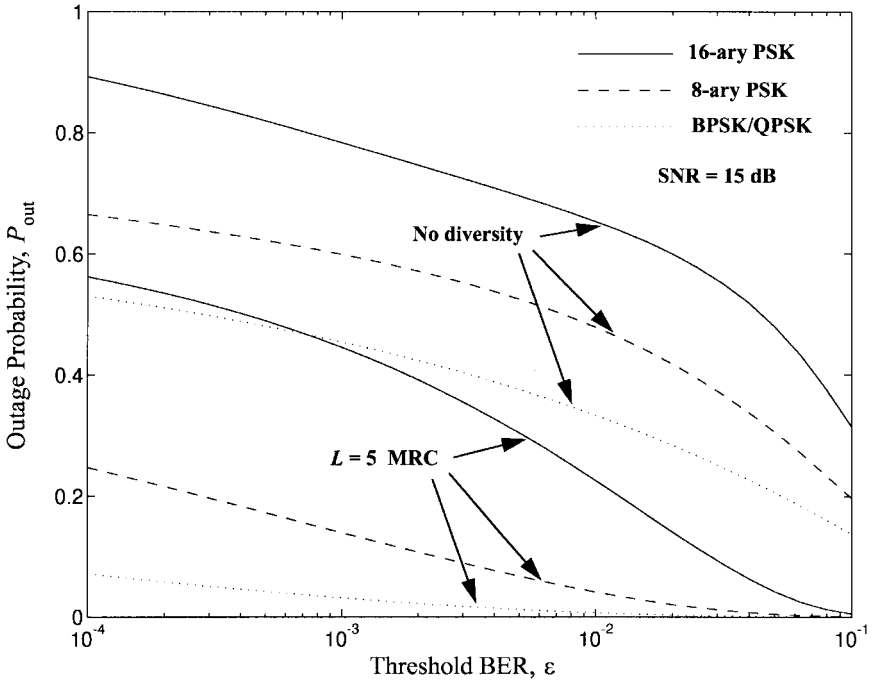

Fig. 7. Outage probability for M-ary PSK ($M = \{2, 4, 8, 16\}$) with MRC microdiversity ($L = \{1, 5\}$) in the Munich city environment.

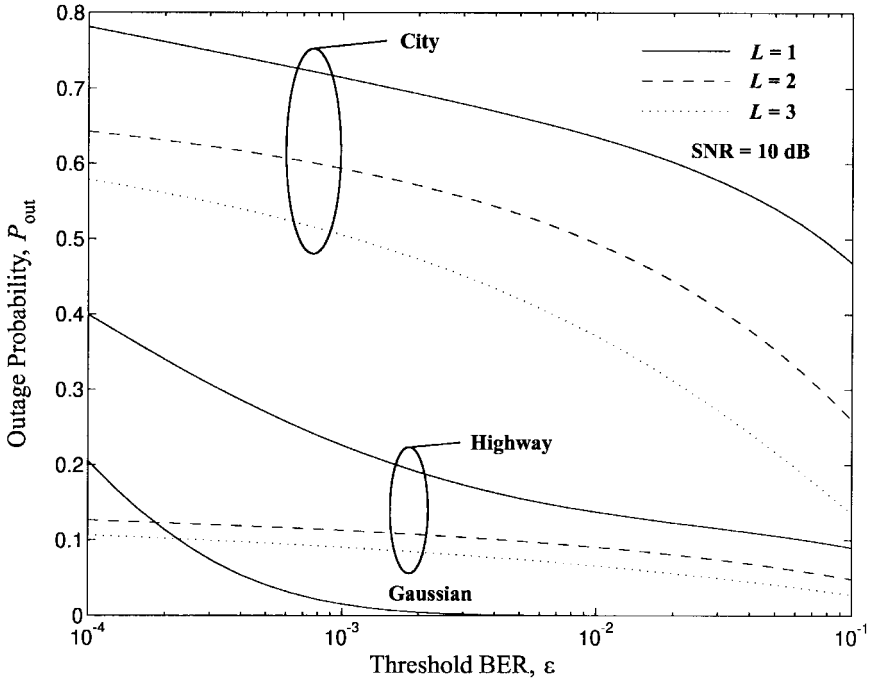

Fig. 8. Outage probability for DPSK with MRC microdiversity ($L = \{1, 2, 3\}$) for the city and highway environments around Munich. The performance of Gaussian (without diversity) is provided for comparison.

is advantageous, as it implies a certain degree of elevation independence for the mobile user.

B. Outage Probability

The outage probability for the Munich city environment for M-ary PSK with and without diversity is shown in Fig. 7. A fixed SNR of 15 dB is assumed. This figure illustrates the significant improvement in coverage, which can be achieved through the use of diversity techniques. For example, at a BER of 10^{-2}, $L = 5$ branch MRC diversity improves the coverage by {3300, 1200, 300}% for $M = \{2$ or $4, 8, 16\}$ PSK. Although not shown, $L = 2$ branch MRC improves the coverage of $M = \{2$ or $4, 8, 16\}$ PSK by {80, 180, 250}%, respectively.

Fig. 8 illustrates the outage probability for DPSK with MRC microdiversity ($L = \{1, 2, 3\}$ for the city and highway

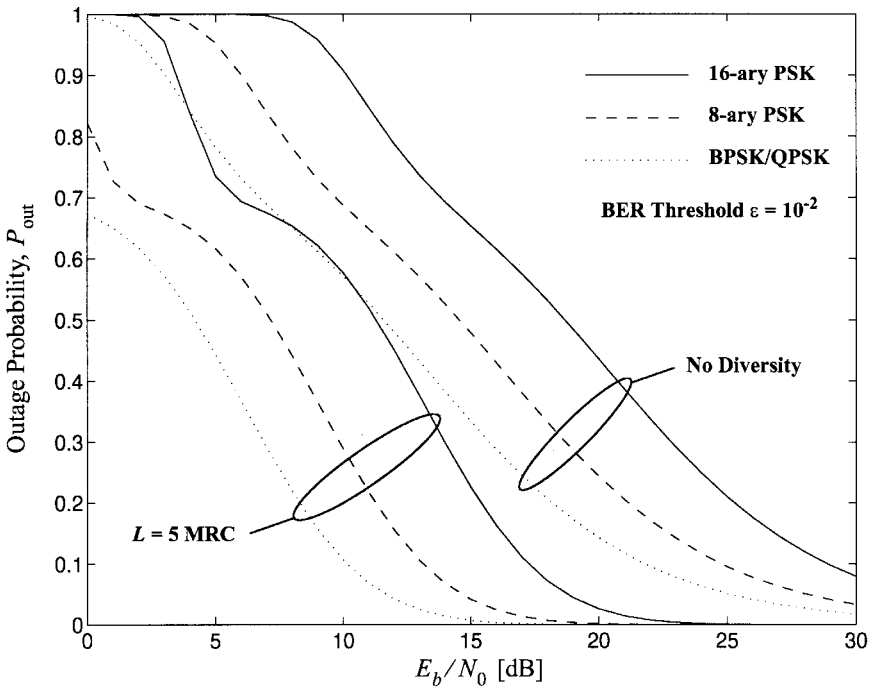

Fig. 9. Outage probability for M-ary PSK with and without $L = 5$ branch MRC microdiversity for Munich city as a function of the SNR. The threshold BER ϵ is fixed to 10^{-2}.

environments around Munich). The effect of shadowing in the city environment is readily seen. Again, microdiversity provides a significant decrease in outage.

Finally, Fig. 9 shows the outage probability for M-ary PSK in the Munich city environment, where $\epsilon = 10^{-2}$ is fixed and the SNR γ is the variable. The distinct elbow for the five-branch MRC case is explained as follows. At low SNR, $P_{\text{out}} \rightarrow 1$ for both channel states. However, as the SNR increases, $P_{\text{out}}^{\text{Rice}} \rightarrow 0$ much quicker than $P_{\text{out}}^{\text{Suzuki}}$. For our case, $P_{\text{out}}^{\text{Suzuki}}$ is still very close to unity when $P_{\text{out}}^{\text{Rice}}$ approaches zero, and thus the elbow occurs at $A = 0.7$ [see (5)]. From this figure, we see that if we require the BER to be less than 10^{-2} at least 90% of the time, then for the nondiversity case we require an SNR of about 22, 25, and 29 dB for $M = \{2 \text{ or } 4, 8, 16\}$ PSK and for the $L = 5$ MRC diversity case we require an SNR of about 10, 13, and 17 dB for $M = 2$ or $4, 8, 16$ PSK.

VII. Conclusion

In this paper, we have presented analytical expressions well suited to numerical analysis for the average BER and outage probability of the LMSC. We considered both coherent and noncoherent M-ary PSK as well as both selection diversity and MRC microdiversity. These expressions are very powerful in that they are functions of the MGF and CDF of the fading channels and can thus be easily adapted to any channel model provided the MGF and CDF are known. We considered a two-state Rician/Suzuki channel model.

Using the measured channel parameters presented in [1], BER and outage probability curves were plotted for various channel environments. Without diversity reception, the BER performance of M-ary PSK for $M > 4$ was sufficiently poor that the more bandwidth-efficient modulation schemes could not be utilized. However, it was shown that diversity reception (especially MRC) provided significant improvements in both the BER and outage probability. In fact, using two-branch MRC diversity, 16-ary PSK outperformed BPSK without diversity. Furthermore, increasing the number of diversity branches reduced the dependency of the average BER and outage probability on the fading environment. Finally, the elevation angle was found to have little effect on the BER performance.

Appendix I
Evaluation of the Remainder Term for Hermitian and Laguerre Integration

We investigate a quasi-analytic approach to the error analysis for both the Hermitian and Laguerre integration methods. For Hermitian integration, the remainder term is [8]

$$|R_n| \leq \frac{n!\sqrt{\pi}}{(2n)!2^n}\left(\max_{-\infty < \zeta < \infty} |f^{2n}(\zeta)|\right) \tag{47}$$

where, for our application, $f(x)$ is given as [see (11)]

$$f(x) = \frac{1}{\sqrt{\pi}} \frac{1}{(1 + z\mu e^{\sqrt{2}\sigma x})^L}. \tag{48}$$

To simplify the evaluation of (47), let $e^{\delta} = z\mu$. Thus, $f(x)$ in (48) can be rewritten as a function of $\sqrt{2}\sigma x + \delta$. Note that the effect of the δ term is to shift the origin of the function, but not its shape and, thus, has no effect on the derivative of $f(x)$. Furthermore, the $\sqrt{2}\sigma x$ term implies that the nth derivative has a factor of $(\sqrt{2}\sigma x)^n$. By this argument, we then have

$$|R_n| \leq \frac{n!(\sqrt{2}\sigma)^{2n}}{(2n)!2^n}\left(\max_{-\infty < \zeta < \infty} |f_1^{2n}(\zeta)|\right) \tag{49}$$

TABLE III
COMPUTED VALUES OF $\phi(n,m)$ USING MAPLE

Order	$L = 1$	$L = 2$	$L = 3$	$L = 4$
$n = 5$	7.3×10^{-4}	2.9×10^{-3}	6.4×10^{-3}	1.0×10^{-2}
$n = 10$	2.4×10^{-4}	1.5×10^{-3}	5.4×10^{-3}	1.6×10^{-2}
$n = 15$	1.0×10^{-1}	1.2×10^{-1}	1.6×10^{-1}	1.8×10^{-1}
$n = 20$	4.6×10^{6}	7.4×10^{6}	7.5×10^{6}	7.6×10^{6}
$n = 25$	6.9×10^{14}	1.1×10^{15}	1.8×10^{15}	2.2×10^{15}

where now

$$f_1(x) = \frac{1}{(1+e^x)^m} \tag{50}$$

which does not depend on z or μ. Let us further write

$$|R_n| \le \phi(n,m)\sigma^{2n} \tag{51}$$

where

$$\phi(n,m) \equiv \frac{n!}{(2n)!}\left(\max_{-\infty<\zeta<\infty}|f_1^{2n}(\zeta)|\right). \tag{52}$$

Using a mathematical evaluation package such as Maple, (52) can be evaluated for the n and L of interest. Table III provides some results. Using this table, the upper bound can be estimated for a given σ. For $\sigma < 4.3$ dB and $L = 1$, $|R_{10}| \le 2.4 \times 10^{-4}$, which is sufficient. For larger σ, the bound on the error term is not sufficiently tight to guarantee a negligible error term. However, this is not to imply that the error term is indeed significant.

Similarly for the Laguerre integration, the remainder term is bounded by [8]

$$|R_n| \le \frac{n!}{(2n)!}\left(\max_{-\infty<\zeta<\infty}|f^{2n}(\zeta)|\right) \tag{53}$$

where in our case [see (15)]

$$f(x) = (1 - Q(\sqrt{2K}, \sqrt{2(1+K)x/z}))^L. \tag{54}$$

Recognizing that can be written as a function of $2(1+K)x/z$, we obtain

$$|R_n| \le \frac{n!}{(2n)!}\left(\frac{2(1+K)}{z}\right)^{2n}\left(\max_{-\infty<\zeta<\infty}|f_1^{2n}(\zeta)|\right) \tag{55}$$

where now

$$f_1(x) = (1 - Q(\sqrt{2K}, \sqrt{x}))^L. \tag{56}$$

Note that since $m(z)$ is needed for larger values of z, the error term appears negligible. Thus, if $z \gg 2(1+K)$, then this approximation becomes very accurate.

APPENDIX II
SIMPSON INTEGRATION

An alternative approach to the Hermitian integration is to truncate the infinite interval to a finite interval and use Simpson integration. Let us write

$$M(z) = \int_a^b e^{-x^2} f(x)\,dx + R_t \tag{57}$$

where $a < 0, b > 0$, $f(x)$ is given by (48) and R_t is the truncation error

$$R_t = \int_b^\infty \frac{e^{-x^2}}{\sqrt{\pi}(1+z\mu e^{\sqrt{2}\sigma x})^L}\,dx + \int_{-a}^\infty \frac{e^{-x^2}}{\sqrt{\pi}(1+z\mu e^{-\sqrt{2}\sigma x})^L}\,dx. \tag{58}$$

To control the total truncation error, both integrals must be less than some tolerance ϵ. Consider first the positive tail for $b < x < \infty$

$$\int_b^\infty \frac{e^{-x^2}}{\sqrt{\pi}(1+z\mu e^{\sqrt{2}\sigma x})^L}\,dx < 0.5\frac{(1-\mathrm{erf}(b))}{(1+z\mu e^{\sqrt{2}\sigma b})^L}. \tag{59}$$

Thus, we need to select b such that this upper bound is less than ϵ. Note that only a crude solution for b is required. Similarly, for the negative tail $(-\infty < x < x)$, a crude upper bound is

$$\int_{-a}^\infty \frac{e^{-x^2}}{(1+z\mu e^{-\sqrt{2}\sigma x})^L}\,dx < \int_{-a}^\infty e^{-x^2} = \frac{(1-\mathrm{erf}(-a))}{2}. \tag{60}$$

Note that this limit is independent of z, σ, and μ. Thus, for $\epsilon \le 2\times10^{-8}$, $a = -4$ is sufficient.

Since the truncation error can be controlled by properly selecting the finite interval, $2n$ point Simpson integration can be used to estimate the finite integral. Select the coordinate sequence such that $x_0 = a$, $x_0 < x_1, \cdots, x_{2n} = b$, with $x_{i+1} - x_i = h$, $i = 0, 1, \cdots, 2n-1$, where $h = (b-a)/(2n)$. The error term is then bounded by

$$|E| \le \frac{(b-a)^5}{2880n^4}\left(\max_{a\le\zeta\le b}|g^4(\zeta)|\right) \tag{61}$$

where $g(x) = \exp(-x^2)f(x)$. Thus, the error term can be made arbitrarily small by choosing large enough n.

ACKNOWLEDGMENT

The authors wish to thank the anonymous reviewers for their useful suggestions and A. Annamalai for his help with the final version of the manuscript.

REFERENCES

[1] D. Cygan, "Analytical evaluation of average bit error rate for the land mobile satellite channel," *Int. J. Sat. Commun.*, vol. 7, pp. 99–102, Apr. 1989.
[2] E. Lutz, D. Cygan, M. Dippold, F. Dolainsky, and W. Papke, "The land mobile satellite communication channel—Recording, statistics, and channel model," *IEEE Trans. Veh. Technol.*, vol. 40, pp. 375–386, May 1991.
[3] J.-P. Linnartz, *Narrowband Land-Mobile Radio Networks*. Norwood, MA: Artech, 1993.
[4] Y. T. Su and J.-Y. Chen, "Cutoff rates of multichannel MFSK and DPSK signals in mobile satellite communications," *IEEE J. Select. Areas. Commun.*, vol. 13, no. 2, pp. 213–221, 1995.
[5] C. K. Pauw and D. L. Schilling, "Probability of error for M-ary PSK and DPSK on a Rayleigh fading channel," *IEEE Trans. Commun.*, vol. 36, pp. 755–756, June 1988.
[6] C. Tellambura, A. J. Mueller, and V. K. Bhargava, "BER and outage probability for the land mobile satellite channel with maximal ratio combining," *Electron. Lett.*, no. 8, pp. 606–608, Apr. 1995.
[7] J. G. Proakis, *Digital Communications*. New York: McGraw-Hill, 1989.
[8] M. Abramovitz and I. A. Stegun, *Handbook of Mathematical Functions*. New York: Dover, 1972.
[9] C. W. Hellstrom, *Elements of Signal Detection and Estimation*. Englewood Cliffs, NJ: Prentice-Hall, 1995.
[10] W. C. Jakes, Ed., *Microwave Mobile Communications*. New York: Wiley, 1974.
[11] R. F. Pawula, S. O. Rice, and J. H. Roberts, "Distribution of the phase angle between two vectors perturbed by Gaussian noise," *IEEE Trans. Commun.*, vol. COM-30, pp. 1828–1841, Aug. 1982.
[12] W. C. Lindsey, "Error probabilities for Rician fading multichannel reception of binary and N-ary signals," *IRE. Trans. Inform. Theory.*, vol. IT-10, pp. 339–350, Oct. 1964.
[13] A. M. D. Turkmani, "Performance evaluation of a composite microscopic plus macroscopic diversity system," *Proc. Inst. Elec. Eng.*, vol. 138, pt. I, no. 1, pp. 15–20, 1991.

C. Tellambura, photograph and biography not available at the time of publication.

A. Joseph Mueller was born in Edmonton, Alta, Canada, in 1967. He received the B.Sc. degree in electrical engineering from the University of Alberta, Edmonton, in 1992 and the M.A.Sc degree in electrical engineering from the University of Victoria, Victoria, B.C., Canada, in 1995.

In December 1995, he joined Digital Dispatch Systems of Richmond, B.C., Canada, as a DSP Design Engineer. Here, he has been involved in the design of wireless modems for the mobile environment. His research interests include bandwidth-efficient modulation schemes, adaptive error control coding, and techniques for combatting the effects of fading channels.

Vijay K. Bhargava (S'70–M'74–SM'82–F'92), photograph and biography not available at the time of publication.